Complexation−Distribution Separated Solvent Extraction Process Designed for Rapid and Efficient Recovery of Inert Platinum Group Metals

Zhiwei Zheng, Tsuyoshi Arai, and Koichiro Takao*

ACCESS | Metrics & More | Article Recommendations | SI Supporting Information

ABSTRACT: Previously, we have demonstrated that thermal-assisted techniques can accelerate the extraction of inert platinum group metals (PGMs), while they still have several concerns about difficulty of temperature control in actual extraction contactors and safety risks arising from heating organic solvents. In this study, we report a complexation−distribution separated extraction process for the accelerated extraction of inert PGMs. This extraction method includes two steps: (1) complexation of PGMs with extractants in aqueous solution and (2) distribution of the formed complex from the aqueous phase to organic one. We separately investigated the complexation and distribution processes for typical inert PGMs such as Ru(III) and Rh(III) in the presence of water-soluble N,N,N',N'-tetra-alkylpyridinediamide ligands (PDA) and bis(trifluoromethylsulfonyl)-amide (Tf_2N^-) counteranions. As a result, the water-soluble complexes of Ru(III) and Rh(III) with PDA can be formed in 0.5 M HNO_3(aq) within 3 h under heating at 356 K. The formed complexes were extracted to the 1-octanol layer containing Tf_2N^- within 5 min at room temperature, where this hydrophobic anion plays an important role to promote extraction of PGMs as an anionic phase-transfer catalyst (PTC). Consequently, we successfully established and demonstrated the complexation−distribution separated extraction process for the accelerated extraction of inert PGMs using a water-soluble ligand and anionic PTC.
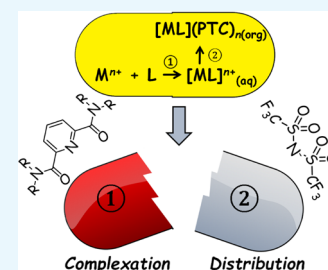
INTRODUCTION

Platinum group metals (PGMs) are highly required in a variety of commercial and industrial applications. This high demand for PGMs will lead to scarcity of resources because of their limited availability from natural environments. To address this issue, recovery of PGMs from wasted materials like electronic devices and automotive catalysts is necessary to be developed.[1−3] In another aspect, several PGMs like Ru(III), Rh(III), and Pd(II) occur in spent nuclear fuels after power generation and may cause a problem in vitrification of high-level radioactive wastes (HLWs).[4,5] Therefore, the development of separation of PGMs is important to make safe and long-term disposal of the nuclear wastes.

The general techniques for recovery and separation of PGMs are pyrometallurgical and hydrometallurgical processes.[6,7] Solvent extraction is a promising hydrometallurgical process and is frequently employed, while extraction of some inert PGMs like Ru(III) and Rh(III) has problems with low recovery efficiency in a realistic operating time. This issue is due to the slow kinetics of the complexation reactions, in accordance with the extremely long lifetime of the water exchange reaction (τ_{H_2O}) of these inert PGMs.[8]

To accelerate the extraction reactions of inert PGMs, we can employ thermal-assisted techniques including microwave irradiation and convection heating, as demonstrated in our previous studies.[9,10] We reported that the extraction of Ru(III) and Rh(III) from HNO_3 aqueous solution (aq) to betainium

bis(trifluoromethylsulfonyl)amide ([Hbet][Tf$_2$N], Figure 1) ionic liquid (IL) took 3.5 and 113 days to reach an

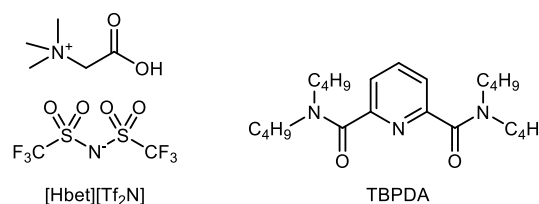**Figure 1.** Schematic structures of [Hbet][Tf$_2$N] and TBPDA.

equilibrium, respectively, at 298 K, while equilibrated within 1 and 3 h at 353 K. This thermal assistance may accelerate the complexation of PGMs with extractants, whereas the formed complex is sometimes difficult to be efficiently partitioned to an organic phase. To improve this situation, we can add an anionic phase transfer catalyst (PTC) like bis-(trifluoromethylsulfonyl)amide (Tf_2N^-, Figure 1).[11] Using

this PTC, the extraction of Ru(III) and Rh(III) in the HNO$_3$(aq)/1-octanol system was promoted to 95 and 90% from 29 and 5%, respectively.

However, employing thermal-assisted techniques in the extraction of inert PGMs will provide some concerns in terms of safety and realistic use. In the thermal-assisted extraction, we have to mix and heat aqueous and organic phases together. This heating treatment involves a high risk because organic solvent normally shows flammability and volatility. Therefore, it is possible to cause fire and poisoning. The other problem is that temperature control of common extraction contactors like mixer−settlers and pulsed columns will not be simple, making the extraction process more complicated.

In this context, we aim to establish and demonstrate a realistic PGM extraction method with thermal assistance for the accelerated extraction of inert PGMs. Although we are aware that selectivity, capacity, and back extraction are also of great interest, the primary solvent extraction process and its fundamentals must be ensured first. Therefore, we report herein extraction behavior of Ru(III) and Rh(III) from HNO$_3$(aq) to 1-octanol. The reasons why we have selected HNO$_3$(aq) herein are (i) it is a practical aqueous system for separation of PGMs from radioactive wastes, and (ii) a simulated feed system should be as simple as possible in terms of coordination chemistry. We are aware that aqueous feed solutions based on HCl(aq) or aqua regia are more popular for recycling PGMs. However, such systems are more challenging compared with HNO$_3$(aq) because the chloro complexation to inert PGMs such as Ru(III) and Rh(III) is much stronger. Here, we select pyridinediamide (PDA) as an extractant in this study because a PDA like N,N,N',N'-tetra-n-butyl-2,6-pyridinediamide (TBPDA, Figure 1) was previously confirmed to present a high potential in the extraction of inert PGMs.[11] We also employ PTC to enhance extraction of inert PGMs in this study.

■ RESULTS AND DISCUSSION

Consideration on Design of the Realistic PGM Extraction Method with Thermal Assistance. To address these concerns about the difficulty of temperature control in actual extraction contactors and safety risks arising from heating organic solvents, we have to further discuss what is an optimal design for a realistic extraction process of the inert PGMs based on the extraction mechanism.

The extraction mechanism can be divided into the following two steps; (1) complexation of M^{n+} with an extractant and (2) distribution equilibrium of the formed complex between aqueous and organic phases, although it is not always easy to know the actual sequence of these reactions in the usual extraction chemistry. The rate-determining step in the PGM extraction must be the complexation step as exemplified by their inertness in the water-exchange reactions.[8] We wonder that the heating treatment in our thermal-assisted extraction is actually required to accelerate this complexation step, and does not largely affect the kinetics of the distribution part. If this hypothesis is correct, we can actually separate these two steps into the different processes, as shown in Figure 2. The first process is designed to prepare a PGM complex with a ligand, [ML$_n$]$^{m+}$, in an aqueous solution, where the thermal assistance is required. Here, both ligand and [ML$_n$]$^{m+}$ must be soluble in the aqueous phase sufficiently. Therefore, we need to design molecular structures of water-soluble ligands. In the next distribution step, the aqueous solution is mixed with an organic
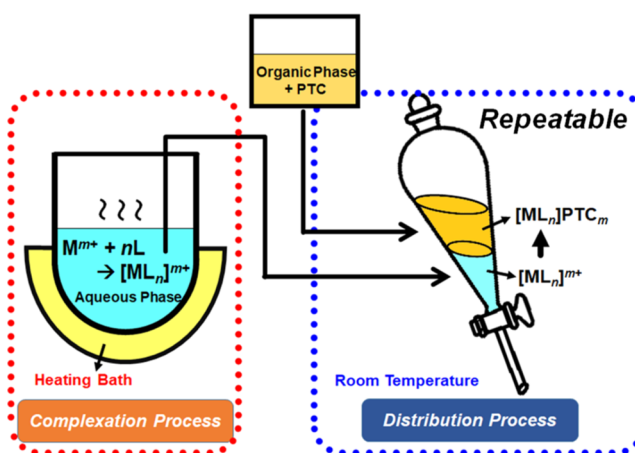

Figure 2. Conceptual artwork of the complexation−distribution separated extraction process for inert PGMs.

phase (e.g., 1-octanol) to extract [ML$_n$]$^{m+}$ formed in the aqueous solution to the organic phase, where the heating treatment is not always necessary. To promote the distribution of PGM from the aqueous phase to the organic one, the positive charge on [ML$_n$]$^{m+}$ formed in this system must be neutralized. Therefore, a hydrophobic counteranion like Tf$_2$N$^-$ should be employed as a charge compensator and a metal carrier to the organic phase, so-called PTC, being demonstrated in our former work.[11] In this complexation−distribution separated extraction process, any organic solvent is no longer necessary to be heated, leading that the safety concerns in the thermal-assisted extraction will be overcome. In addition, the technical problems arising from the difficulty in temperature control of the actual extraction contactors will also be resolved.

The first task in this study is molecular design of water-soluble ligands because TBPDA (Figure 1) we used previously is strongly hydrophobic and only soluble by 1.3 mM in HNO$_3$(aq). Here, we decided to shorten the terminal alkyl chains of PDA, as shown in Figure 3, to increase its
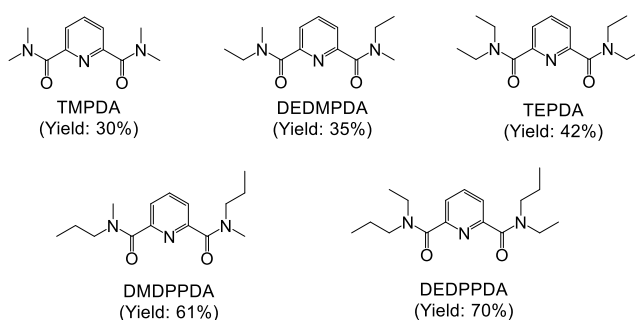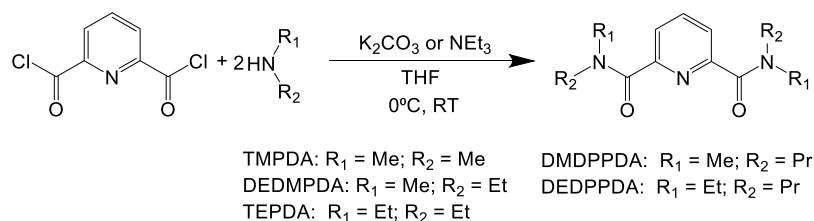

Figure 3. Schematic structures of several water-soluble ligands related to this work.

hydrophilicity to solubilize a ligand molecule and its PGM complex in an aqueous phase. Such a water-soluble ligand may provide difficulty in the actual extraction of PGMs due to the lower lipophilicity of its complex formed in the aqueous phase. To resolve this problem, charge compensation with a hydrophobic PTC anion will facilitate the extraction of PGMs coordinated with the water-soluble ligand. In the next sections, we are going to examine step-by-step whether or not our concept described above indeed works well in the actual

Scheme 1. Preparation of PDA Ligands

TMPDA: R_1 = Me; R_2 = Me   DMDPPDA: R_1 = Me; R_2 = Pr
DEDMPDA: R_1 = Me; R_2 = Et   DEDPPDA: R_1 = Et; R_2 = Pr
TEPDA: R_1 = Et; R_2 = Et

extraction chemistry of the typical inert PGMs such as Ru(III) and Rh(III).

Synthesis and Characterization of Water-Soluble Ligands. Various water-soluble PDA ligands, as shown in Figure 3, were synthesized through a reaction between 2,6-pyridinedicarbonyl dichloride and a secondary amine in the presence of K_2CO_3 or NEt_3 in tetrahydrofuran (THF), as described in Scheme 1. Consequently, TMPDA was obtained as white powder, whereas DEDMPDA, TEPDA, DMDPPDA, and DEDPPDA were afforded as slightly yellow oil or solid. All PDA ligands were identified by ^{1}H and ^{13}C{^{1}H} NMR and IR spectroscopy, as shown in Figures S1−S20. In the ^{1}H NMR spectra of DEDMPDA, DMDPPDA, and DEDPPDA, all the terminal alkyl chains are not chemically equivalent (see Figures S6, S14, and S18), suggesting that these ligands do not have any 2-fold axes in their actual molecular structures, as shown in Figure 3.

The hydrophobicity of these PDA ligands was estimated in terms of the logarithmic partition coefficient (log P) in the 0.5 M HNO_3(aq)/1-octanol system.[12,13] Furthermore, the solubility of these PDA ligands in 0.5 M HNO_3(aq) was also quantified from the ^{1}H NMR spectra of the saturated solutions. The results are summarized in Table 1 together with those of

Table 1. Logarithmic Partition Coefficients of PDA Ligands (log P) in the 0.5 M HNO_3(aq)/1-Octanol System and Solubility of PDA Ligands in 0.5 M HNO_3(aq)

ligand	log P	solubility/M
TMPDA	−1.460	2.25
DEDMPDA	−0.610	1.58
TEPDA	0.308	0.55
DMDPPDA	0.689	fully miscible
DEDPPDA	0.980	0.40
TBPDA	1.315	0.0013

TBPDA. Note that the solubility of DMDPPDA cannot be determined because this oily material is fully miscible with 0.5 M HNO_3(aq). The resulting solubility data indicate that all of the PDA ligands prepared here are water-soluble enough to be utilized in the complexation−distribution separated extraction process we proposed in Figure 2.

Thermal Acceleration of the Complexation Process of Ru(III) and Rh(III) in the Aqueous Phase. In the next step, the complexation of Ru(III) and Rh(III) with PDA in HNO_3(aq) was investigated by means of ultraviolet−visible (UV−vis) absorption spectroscopy. In this process, we intended to know whether a water-soluble M−PDA [M = Ru(III) and Rh(III)] complex is indeed formed and to clarify how long this reaction actually takes. We selected TMPDA as a ligand because it is a white powder, and therefore, suitable for this spectroscopic study.

Ru(III) (5 mM) or Rh(III) (1.5 mM) was dissolved in 0.5 M HNO_3(aq) with TMPDA (30 mM) at 356 K, followed by recording UV−vis absorption spectra of this solution every 30 min. As shown in Figure 4a, the intensity of the characteristic
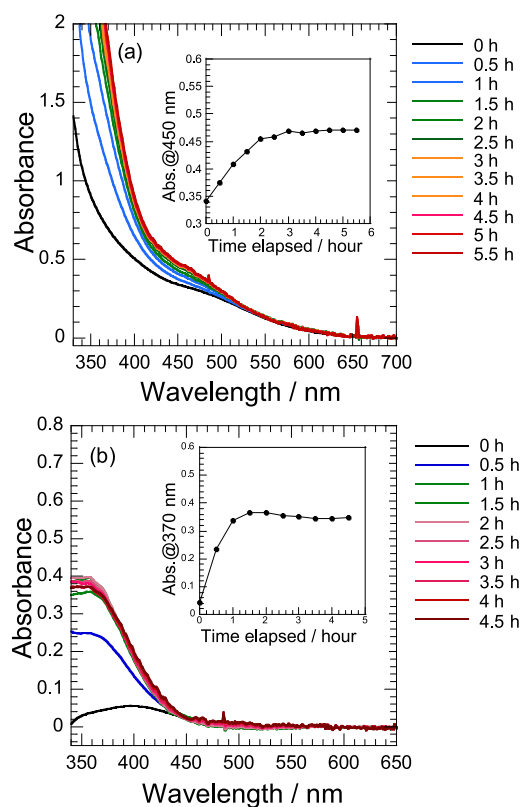

Figure 4. UV−vis absorption spectra of 0.5 M HNO_3(aq) containing 5 mM Ru(III) (a) or 1.5 mM Rh(III) (b) with 30 mM TMPDA at 356 K. Inset: progress of absorbance at 450 nm [Ru(III)] and 370 nm [Rh(III)] at 356 K with elapse of time.
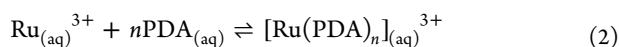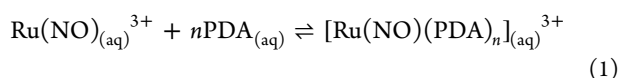
absorption band of Ru(III) at 450 nm increased with elapse of time and reached equilibrium within 3 h. These results indicate that the complexation process of Ru(III) with TMPDA reaches equilibrium within 3 h. The observed apparent first-order rate constant (k_{obs}) of the complexation of Ru(III) with TMPDA at 356 K was evaluated to be 2.2×10^{-4} s^{-1} from the exponential curve for absorbance at 450 nm as a function of elapse of time, as shown in Figure S21a. In addition, the nitrosyl ligand (NO) should still remain coordinated to the center Ru^{3+} even after the complexation with TMPDA because the typical absorption band in the range of 380−400 nm has always appeared through the recorded UV−vis spectral series, as shown in Figure 4a.[14]

A similar result was also obtained in the Rh(III) system, as shown in Figure 4b. The intensity of the absorption band centered at 370 nm increased with elapse of time and reached

equilibrium within 2 h. The k_{obs} value of the complexation of Rh(III) with TMPDA at 356 K was estimated to be 6.3×10^{-4} s^{-1}, as shown in Figure S21b. Consequently, we have confirmed that the water-soluble M−PDA complexes [M = Ru(III) and Rh(III)] can be formed in 0.5 M HNO$_3$(aq) as expected.

Additionally, we also investigated the complexation reactions of Ru(III) and Rh(III) with TMPDA at 298 K, as shown in Figure S22. As a result, we did not observe any change in the absorption spectra of Ru(III) and Rh(III) up to 5 h. These results indicate that the complexation reactions of Ru(III) and Rh(III) with TMPDA do not proceed at 298 K practically. The difference between the kinetic aspects at 356 and 298 K demonstrated that elevating temperature efficiently promotes the complexation reactions of Ru(III) and Rh(III) with TMPDA.

The complexation equilibria, as observed in Figure 4, can be postulated as follows.

$$\text{Ru(NO)}_{(aq)}^{3+} + n\text{PDA}_{(aq)} \rightleftharpoons [\text{Ru(NO)(PDA)}_n]_{(aq)}^{3+} \tag{1}$$

$$\text{Ru}_{(aq)}^{3+} + n\text{PDA}_{(aq)} \rightleftharpoons [\text{Ru(PDA)}_n]_{(aq)}^{3+} \tag{2}$$

where the subscripted "(aq)" indicates the location of a species. The details in the stoichiometry of each reaction will be assessed in a mechanistic discussion described later.

Distribution Process of Ru(III) and Rh(III) from the Aqueous Layer to the Organic Phase at Room Temperature. Based on the results of UV−vis absorption spectroscopy, we next investigated the distribution process of the M−PDA complexes [M = Ru(III) and Rh(III)] from the 0.5 M HNO$_3$(aq) layer to the 1-octanol phase. First, a mixture of M [5 mM, M = Ru(III) and Rh(III)] and a water-soluble PDA ligand (30 mM, Figure 3) in 0.5 M HNO$_3$(aq) was heated at 356 K for 5 h. This reaction time is long enough to complete the complexation process of Figure 2, as demonstrated in the former section. After that, this aqueous solution was shaken with 1-octanol containing 500 mM LiTf$_2$N at room temperature (RT), where LiTf$_2$N was employed to provide Tf$_2$N$^-$ as an anionic PTC, in accordance with our former work.[11] We have continued shaking the aqueous and organic phases up to 2 h in the distribution experiments. As a result, extractabilities were not different from those at 5 min. Therefore, we concluded that 5 min is long enough to reach the distribution equilibria in the systems tested here.

As shown in Figure 5, the extractability (E %) of Ru(III) and Rh(III) was plotted as a function of log P of the PDA ligands. As a general trend, E % of both Ru(III) and Rh(III) increases with an increase in the hydrophobicity of the PDA ligand pronounced by log P. For instance, the least-hydrophobic ligand, TMPDA (log P = −1.460), gave the lowest E % of Ru(III) (17%) and Rh(III) (15%). In contrast, DEDPPDA, the most-hydrophobic (log P = 0.980) in the ligands tested here, afforded much higher E % such as 72 and 48% for Ru(III) and Rh(III), respectively. This contrast clearly indicates that the difference in hydrophobicity arising from the alkyl substituents of PDA ligands strongly affects E % of Ru(III) and Rh(III). DEDPPDA does not simply show the highest E % only in the PDA ligands tested here but is also more efficient for Ru(III) and Rh(III) extraction from HNO$_3$(aq) compared with other extractants like an amino acid derivative bearing a polyalkylated-aminocarbonyl group, tri-n-butyl phosphate, and tri-isooctylamine in ordinary organic
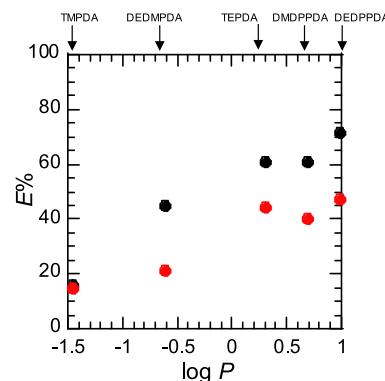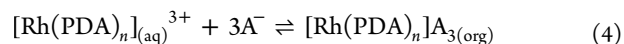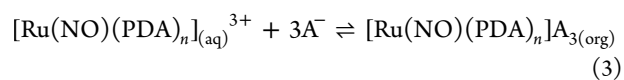

Figure 5. Extractability (E %) of Ru(III) (black) and Rh(III) (red) as a function of log P of the PDA ligand in the 0.5 M HNO$_3$(aq)/1-octanol system. Experiment processes and conditions: the HNO$_3$(aq) containing 5 mM M [M = Ru(III) and Ru(III)] and 30 mM PDA was heated at 356 K for 5 h. After cooling to RT, the aqueous solution was stirred at RT for 5 min with 1-octanol containing 500 mM LiTf$_2$N. E % was derived from the initial and final concentrations of each PGM in the aqueous phases.

solvent systems.[15,16] In these former systems, E % from HNO$_3$(aq) was up to *ca.* 10% or less. Although extraction mechanisms are not always fully clarified, we wonder that inertness of these PGMs in ligand substitution reactions is one of the main reasons of such inefficient extraction, as we pointed out in the introduction section. Higher E % of Ru(III) and Rh(III) can be actually achieved using ILs as alternative non-aqueous phases.[9,10,17,18] However, much higher cost and difficulty in handling due to higher viscosity compared with ordinary organic solvents are main critical drawbacks of ILs in the solvent extraction. Our current work successfully demonstrated that the solvent extraction of Ru(III) and Rh(III) from HNO$_3$(aq) can be facilitated even using an ordinary organic solvent like 1-octanol. In addition, E % of Rh(III) was lower than that of Ru(III) using the same PDA ligand, resulting in the different distribution ratio of M−PDA complexes [M = Ru(III) and Rh(III)] in the 0.5 M HNO$_3$(aq)/1-octanol system.

Consequently, the complexation−distribution separated extraction process we proposed in Figure 2 is successfully demonstrated for the solvent extraction of Ru(III) and Rh(III) from HNO$_3$(aq) to 1-octanol using appropriately selected PDA as the water-soluble ligand and Tf$_2$N$^-$ as an anionic PTC hydrophobic enough. This extraction process overcomes the difficulty of temperature control in actual extraction contactors and safety risks arising from heating organic solvents in the thermal-assisted extraction proposed in our previous studies.[9−11] In connection with eqs 1 and 2, the distribution equilibria, as shown in Figure 5, can be postulated as follows.

$$[\text{Ru(NO)(PDA)}_n]_{(aq)}^{3+} + 3\text{A}^- \rightleftharpoons [\text{Ru(NO)(PDA)}_n]\text{A}_{3(org)} \tag{3}$$

$$[\text{Rh(PDA)}_n]_{(aq)}^{3+} + 3\text{A}^- \rightleftharpoons [\text{Rh(PDA)}_n]\text{A}_{3(org)} \tag{4}$$

where the subscripted "(aq)" and "(org)" indicate the location of a species. A$^-$ denotes a counteranion like Tf$_2$N$^-$ and NO$_3^-$, which makes an ion pair with [Ru(NO)(PDA)$_n$]$^{3+}$ or [Rh(PDA)$_n$]$^{3+}$ to compensate electric charge balance in both aqueous and organic phases. Note that the addition of Tf$_2$N$^-$ as an anionic PTC is required to enhance E % of PGMs by compensating the positive charge of the extractable species.

This significant impact has already been confirmed in our former work.[11] The details how $[Tf_2N^-]$ affects the extraction chemistry of the current system will be described in the later discussion about extraction mechanisms.

Reaction Mechanisms of Ru(III) and Rh(III) in the Complexation–Distribution Separated Extraction Process. Our next concern is to clarify the extraction mechanisms of the inert PGMs in the studied systems. Although the coordination chemistry of Ru^{3+} in $HNO_3(aq)$ is quite complicated,[19,20] a Ru(III) species is believed to be present as a nitrosyl species like $Ru(NO)^{3+}$, as suggested spectroscopically in Figure 4a. Rh(III) in an aqueous solution is believed to be present as $[Rh(H_2O)_6]^{3+}$ even in the presence of 0.5 M HNO_3.[21]

To determine the stoichiometry of the PDA ligand in eqs 1 and 2, we investigated the effect of the ligand concentration on the extraction of $Ru(NO)^{3+}$ and Rh^{3+}. Here, we selected TEPDA for this purpose because this ligand exhibits relatively high E % of $Ru(NO)^{3+}$ and Rh^{3+}, as shown in Figure 5. Figure 6 shows plots of E % of $Ru(NO)^{3+}$ and Rh^{3+} as a function of
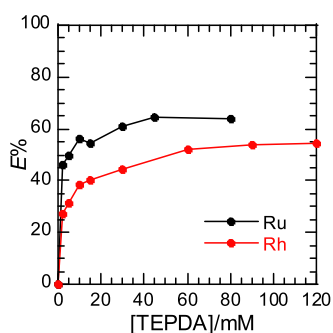

Figure 6. Effect of the concentration of TEPDA on $Ru(NO)^{3+}$ and Rh^{3+} extraction from 0.5 M $HNO_3(aq)$ to 1-octanol. The experimental procedure is as following: $HNO_3(aq)$ solution containing 5 mM $Ru(NO)^{3+}$ or Rh^{3+} with 2−120 mM TEPDA was heated at 356 K for 5 h, followed by cooling and mixing with 1-octanol dissolving 500 mM $LiTf_2N$ for 5 min at RT.

[TEPDA]. As a result, E % of $Ru(NO)^{3+}$ and Rh^{3+} first increased with an increase in [TEPDA] and then reached the plateau region at 64 and 52%, respectively. In the usual extraction chemistry, an ordinary approach to determine the stoichiometry of a ligand bound to a metal ion is the slope analysis of the full logarithmic plot of the distribution ratio (log D) as a function of the ligand concentration. Figure S23 shows that the slopes of the best fit line for log D as a function of log[TEPDA] were estimated to be 0.22 and 0.37 for $Ru(NO)^{3+}$ and Rh^{3+}, respectively. Nevertheless, these slopes do not meet any reliable stoichiometry of ligands. To express this situation, we have to further discuss the results, as shown in Figure 6.

The plateau region of E %, as shown in Figure 6, implies that complexation reactions in eqs 1 and 2 have predominantly proceeded in the aqueous solution, when [TEPDA] is high enough. In the following distribution step, we have simply observed the partitioning of the formed complexes $[Ru(NO)-(TEPDA)_n]^{3+}$ and $[Rh(TEPDA)_n]^{3+}$ between the aqueous and organic phases, as shown in eqs 3 and 4. Note that no term of [TEPDA] appears in these distribution processes because of completion of the complexation and inertness of these PGMs, as demonstrated in the kinetic study described above.

Therefore, slope analysis frequently employed in usual solvent extraction studies is not suitable to determine the stoichiometry in the current systems. However, the stoichiometric information must be involved in the observed trends, as shown in Figure 6. Consequently, we decided to take another approach to clarify the ligand stoichiometry in eqs 1 and 2 in terms of sensitivity of estimated stability constants of the $[M(TEPDA_n)]^{3+}$ complexes toward different n.

For better understanding, the complexation and distribution processes are simplified as follows.

Complexation process:

$$M_{(aq)} + nL_{(aq)} = ML_{n(aq)} \tag{5}$$

Distribution process:

$$ML_{n(aq)} + 3A = [ML_n](A)_{3(org)} \tag{6}$$
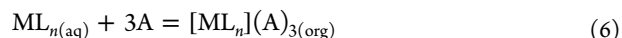
where M, L, and A are a metal ion, ligand, and counteranion, respectively. Charges of M and A are omitted for clarity. We have already known the concentrations of M (C_M^{ini}) and L (C_L^{ini}) initially loaded to the aqueous phase. Note that E % of the $[ML_n]$ complexes should be always constant at those points in the plateau region observed in Figure 6 [E %$_{pl}$: 64% for $Ru(NO)^{3+}$, 52% for Rh^{3+}]. Therefore, the total concentrations of the $[ML_n]$ complexes actually formed in the aqueous phase at the complexation process of Figure 2 ($C_{ML_n}^{com}$) can be calculated as follows.

$$C_{ML_n}^{com} = (C_{Morg}^{dis})/(E\,\%_{pl}/100)$$
$$= (C_M^{ini} - C_{Maq}^{dis})/(E\,\%_{pl}/100) \tag{7}$$

where C_{Morg}^{dis} and C_{Maq}^{dis} denote concentrations of M present in the organic and aqueous phases after the distribution process, as shown in Figure 2, respectively. The latter is directly determined by inductively coupled plasma atomic emission spectroscopy (ICP-AES) in the experiments of Figure 6. Accordingly, the concentrations of non-coordinated M (C_M^{com}) and free L (C_L^{com}) in the aqueous phase at the complexation process are evaluated as

$$C_M^{com} = C_M^{ini} - C_{ML_n}^{com} \tag{8}$$

$$C_L^{com} = C_L^{ini} - nC_{ML_n}^{com} \tag{9}$$

As a result, the gross stability constants of the $[ML_n]$ complexes (β_n) in the aqueous solution of the complexation process can be expressed as follows.

$$\beta_n = (C_{ML_n}^{com})/(C_M^{com}C_L^{com\,n}) \tag{10}$$

If the stoichiometry of L (n) in eq 5 is correctly postulated, β_n should be constant regardless of the difference in C_L^{ini}. Taking into account the possible total coordination numbers around the Ru^{3+} and Rh^{3+} centers up to 6 and tridentate coordination manner of the PDA ligand, n would be 1 or 2.

Using eqs 7−10, logarithmic β_n (log β_n) of [Ru(NO)-(TEPDA)$_n$]$^{3+}$ and [Rh(TEPDA)$_n$]$^{3+}$ at different C_L^{ini} of TEPDA was calculated, as summarized in Table S1. Assuming n = 1, log β_1 of [Ru(NO)(TEPDA)]$^{3+}$ and [Rh(TEPDA)]$^{3+}$ complexes was evaluated to be 3.04 ± 0.58 and 2.54 ± 0.41, respectively. When n = 2, log β_2 of [Ru(NO)(TEPDA)$_2$]$^{3+}$ and [Rh(TEPDA)$_2$]$^{3+}$ was estimated to be 5.52 ± 1.48 and 5.13 ± 1.67, respectively. These results indicate that the stoichiometry of TEPDA (n) in both eqs 1 and 2 should be 1. The formation

Scheme 2. Predictable Stepwise Hydrolysis Reactions of PDA under Acidic Conditions
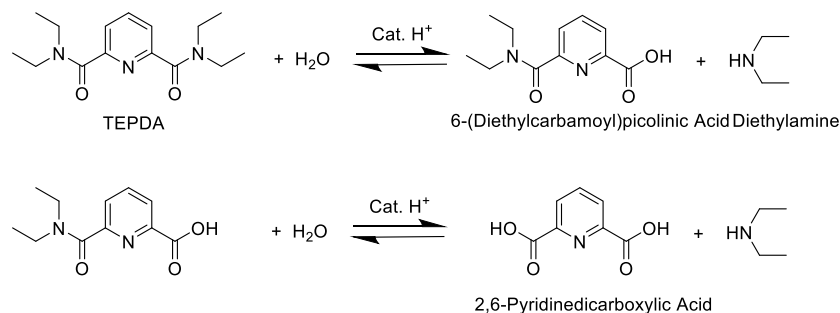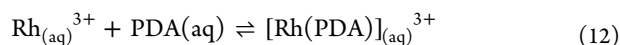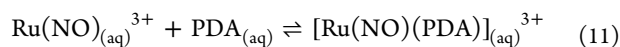

of 1:1 complexes is also in line with that using TBPDA (Figure 1) we reported previously.[11] Therefore, this stoichiometry seems to be common to these inert PGMs with the PDA ligands.
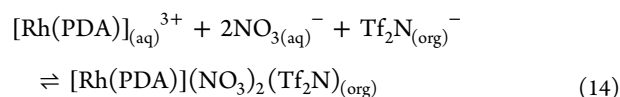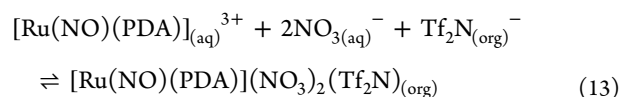
Our next task is to clarify the stoichiometry of counteranion in eqs 3 and 4. In the current system, the possible counteranions are Tf_2N^- and NO_3^-. First, we studied the dependency of log D of $Ru(NO)^{3+}$ and Rh^{3+} on $\log[Tf_2N^-]$ using TEPDA, as shown in Figure S24. As a result, log D of $Ru(NO)^{3+}$ and Rh^{3+} increased with an increase in $[Tf_2N^-]$. These results indicate that employing an anionic PTC like Tf_2N^- can actually enhance the extraction of $Ru(NO)^{3+}$ and Rh^{3+} in this study. The slopes of the best fit line were evaluated to be 1.09 and 0.81 for $Ru(NO)^{3+}$ and Rh^{3+}, respectively, indicating that the stoichiometry of Tf_2N^- in both eqs 3 and 4 seems to be close to 1. After involving the Tf_2N^-, the ion-pairs, $\{[Ru(NO)(TEPDA)]Tf_2N\}^{2+}$ and $\{[Rh(TEPDA)]Tf_2N\}^{2+}$, still have two positive charges which must be compensated through the extraction. NO_3^- is only available as another counteranion present in this system. Therefore, two NO_3^- should be involved in the actual distribution process. We have previously studied the slope of the best fit line for log D of $Ru(NO)^{3+}$ as a function of $\log[NO_3^-]$ using TBPDA.[11] However, the slope did not meet the expected stoichiometry of NO_3^- because the activity coefficient of each species should be strongly affected by the wide variation of ionic strength from a large range of $[NO_3^-]$.

In summary, we conclude that the complexation−distribution separated extraction of $Ru(NO)^{3+}$ and Rh^{3+} in $HNO_3(aq)$/1-octanol system proceeds through the following reaction mechanisms.

Complexation process:

$$Ru(NO)_{(aq)}{}^{3+} + PDA_{(aq)} \rightleftharpoons [Ru(NO)(PDA)]_{(aq)}{}^{3+} \quad (11)$$

$$Rh_{(aq)}{}^{3+} + PDA(aq) \rightleftharpoons [Rh(PDA)]_{(aq)}{}^{3+} \quad (12)$$

Distribution process:

$$[Ru(NO)(PDA)]_{(aq)}{}^{3+} + 2NO_{3(aq)}{}^- + Tf_2N_{(org)}{}^-$$
$$\rightleftharpoons [Ru(NO)(PDA)](NO_3)_2(Tf_2N)_{(org)} \quad (13)$$

$$[Rh(PDA)]_{(aq)}{}^{3+} + 2NO_{3(aq)}{}^- + Tf_2N_{(org)}{}^-$$
$$\rightleftharpoons [Rh(PDA)](NO_3)_2(Tf_2N)_{(org)} \quad (14)$$

Stability of PDA Ligands in $HNO_3(aq)$ and Impact on Coordination and Extraction Chemistry of Ru(III) and Rh(III). Up to now, we have successfully demonstrated the extraction of the inert PGMs such as $Ru(NO)^{3+}$ and Rh^{3+}, as

we proposed in Figure 2. Nevertheless, we still had a concern about the stability of the PDA ligand because the carbon−nitrogen bond of PDA could be broken in $HNO_3(aq)$ especially under heating treatment. Scheme 2 shows the possible reaction scheme of stepwise decomposition of PDA through H^+-catalyzed hydrolysis of the amide moieties.

To assess this issue, TEPDA in 0.5 M $HNO_3(aq)$ was heated at 356 K, followed by recording ^1H NMR spectra of this solution at 0, 2, 5, 23, and 46 h. The obtained results are shown in Figure S25a,b together with ^1H NMR spectra of 2,6-pyridinedicarboxylic (c) acid and diethylamine (d) in 0.5 M $HNO_3(aq)$ as predictable decomposition products. As a result, we observed that signal intensities at 1.04, 2.83, 7.66, 8.10, 8.15, and 8.23 ppm gradually increased with elapse of time, as shown in Figure S25a,b. These signals can be associated to 2,6-pyridinedicarboxylic acid (8.15 and 8.23 ppm) and diethylamine (1.04 and 2.83 ppm) afforded by hydrolysis of TEPDA, in accordance with Figure S25c,d. Another set of ^1H NMR signals detected at 7.66 and 8.10 ppm can be assigned to 6-(diethylcarbamoyl)picolinic acid. This species can be assigned to the product of the first hydrolysis of TEPDA. Although its reference spectrum is not available, its appearance prior to that of 2,6-pyridinedicarboxylic acid is in line with the stepwise decomposition, as shown in Scheme 2. This result indicates that the hydrolysis reaction of TEPDA actually proceeds in $HNO_3(aq)$ even in the absence of metal ions at 356 K.

Now, we wonder whether or not such hydrolysis reactions have to be considered in the formation of $[Ru(NO)-(TEPDA)]^{3+}$ and $[Rh(TEPDA)]^{3+}$ in our complexation process followed by solvent extraction. To confirm the stability of $[Ru(NO)(TEPDA)]^{3+}$ and $[Rh(TEPDA)]^{3+}$, we assessed the thermal stability of TEPDA (30 mM) in 0.5 M $HNO_3(aq)$ in the presence of 5 mM $Ru(NO)^{3+}$ or Rh^{3+} in a similar manner to Figure S25. The obtained ^1H NMR spectra are shown in Figures S26 and S27 for $Ru(NO)^{3+}$ and Rh^{3+} systems, respectively. As a result, we observed that a signal intensity at 2.83 ppm of diethylamine slightly increased with elapse of time, indicating that the hydrolysis reaction of TEPDA indeed proceeds in $HNO_3(aq)$ in the presence of $Ru(NO)^{3+}$ or Rh^{3+}. However, the concentrations of this decomposition product estimated from the peak integrals were 2.4 mM at 3 h (Figure S26) and 1.8 mM at 2 h (Figure S27) in the presence of $Ru(NO)^{3+}$ and Rh^{3+}, respectively. These results indicate decomposition of 1.2 and 0.9 mM TEPDA, which are still smaller than that of the metal concentrations (5 mM) loaded to these samples. As shown in Figure 4a, we have already confirmed that complexation of $Ru(NO)^{3+}$ with TMPDA is completed within 3 h and remains unchanged up to 5.5 h. We also demonstrated that complexation of Rh^{3+} with TMPDA is completed within 2 h and remains unchanged up to

4.5 h, as shown in Figure 4b. We believe that the difference in the terminal alkyl chain lengths of TEPDA and TMPDA is unlikely to strongly affect coordination chemistry of M^{3+} [M = Ru(NO) and Rh] and hydrolytic decomposition of these extractants in the current systems. Consequently, we have confirmed that TEPDA is gradually hydrolyzed in $HNO_3(aq)$ under heating at 356 K, whereas such hydrolysis does not have any impact on formation of $[Ru(NO)(TEPDA)]^{3+}$ and $[Rh(TEPDA)]^{3+}$ and their extraction chemistry in the current systems.

When the sample solution of Figure S26 was kept for several weeks at RT, we observed deposition of brown crystals in the NMR tube. The crystal structure was determined using the single-crystal X-ray diffraction method. As shown in Figure S28, one 2,6-pyridinedicarboxylated, one 6-(diethylcarbamoyl)picolinate, and one nitrosyl are bound to the Ru^{3+} center to give an octahedral complex, while we did not find the parent TEPDA itself in this complex. This result implies that TEPDA is indeed hydrolyzed upon long contact with $HNO_3(aq)$.

Demonstration of Multistage Extraction of Ru(III) and Rh(III) Mixtures. After single-stage extraction of Ru(III) and Rh(III) was confirmed, we next intended to demonstrate feasibility and extendability of the complexation−distribution separated extraction process (Figure 2) to a more practical multistage extraction process. Both $Ru(NO)^{3+}$ and Rh^{3+} (5 mM each) were dissolved in 0.5 M $HNO_3(aq)$ with DEDPPDA (30 mM), followed by heating at 356 K for 5 h to complete the complexation process. Herein, we selected DEDPPDA because it gave the highest $E\%$ of $Ru(NO)^{3+}$ and Rh^{3+}, as shown in Figure 5. After completion of the complexation process, this aqueous phase was vigorously shaken with 1-octanol containing 500 mM $LiTf_2N$ at RT. After separation of the organic layer, the aqueous phase was again contacted with a fresh organic solvent having the same composition with that used in the first cycle. The distribution process was repeated four times to examine the efficiency of the multistage extraction. Figure 7 shows the cumulative $E\%$ ($E\%_{cum}$) of $Ru(NO)^{3+}$ and Rh^{3+} as a function of extraction stages. As a result, $E\%_{cum}$ of $Ru(NO)^{3+}$ and Rh^{3+} increased with an increase in the number of extraction cycles. After the fourth cycle, $E\%_{cum}$ of $Ru(NO)^{3+}$ and Rh^{3+} reached up to 97

and 92%, respectively. These results indicate that the complexation−distribution separated extraction process, as shown in Figure 2, is indeed appropriate for multistage extraction. Moreover, to compare the single and multistage extraction experiments, the open symbols, as shown in Figure 7, denote the ideal $E\%_{cum}$ of $Ru(NO)^{3+}$ and Rh^{3+} in each extraction stage calculated from the result of single-stage extraction, as shown in Figure 5 [$E\%$ in each stage: 72% for $Ru(NO)^{3+}$ and 48% for Rh^{3+}]. As a result, actual and predicted $E\%_{cum}$ of $Ru(NO)^{3+}$ and Rh^{3+} at each extraction stage are very close to each other, indicating that interference between $Ru(NO)^{3+}$ and Rh^{3+} is negligible even in the multistage extraction. In addition, actual feed solutions such as HLW generated from the reprocessing process for spent nuclear fuels do not contain only PGMs but also other fission products and minor actinides. At this moment, we do not assess selectivity toward PGMs in the current $HNO_3(aq)$ system because PDA has not been chosen as a promising extractant for mutual separations in the actual HLW treatment. There is still much space to select or improve ligand molecular structures to design better extractants on demand of separation and recovery. Our main focus in this study is to confirm the feasibility of the complexation−distribution separated extraction process, as shown in Figure 2, which has been successfully demonstrated, as described above. This makes a solvent extraction process more realistic even for inert metal ions like Rh(III) and Ru(III).

CONCLUSIONS

In this study, we designed and demonstrated a complexation−distribution separated extraction process for the accelerated extraction of inert PGMs. We have confirmed that the water-soluble $[M(PDA)]^{3+}$ complexes [M = Ru(NO) and Rh] can be successfully formed in 0.5 M $HNO_3(aq)$ under heating treatment. The $[M(PDA)]^{3+}$ complexes in the aqueous phase were rapidly and efficiently extracted to the 1-octanol layer at RT within 5 min. The actual forms of extractable species would be $[M(PDA)](NO_3)_2(Tf_2N)$ [M = Ru(NO) and Rh], where Tf_2N^- significantly enhances the solvent extraction as an anionic PTC. This concept of extraction we proposed here overcomes the problems of safety risks and temperature control in the actual solvent extraction process of chemically inert species and significantly expands the application of our thermal-assisted techniques. As our next tasks, we further investigate the coordination and structural chemistry of extractable species in the current extraction system. Back extraction of PGMs from the organic phase to aqueous phase is also of interest in the next step. Possible methods like removing PTC or employing hydrophilic PTC will be investigated. Furthermore, molecular design of water-soluble ligands should be improved to make them more chemically stable toward hydrolysis. We intend to expand applicability of this complexation−distribution separated method to the solvent extraction of PGMs from HCl(aq), a more practical aqueous system for precious metals recycling from their social stocks so-called urban mining.

Figure 7. Actual and calculated total extractability ($E\%$) of $Ru(NO)^{3+}$ and Rh^{3+} as a function of extraction cycles in 0.5 M $HNO_3(aq)$/1-octanol system. The experimental procedure is as following: 0.5 M $HNO_3(aq)$ solution containing 5 mM $Ru(NO)^{3+}$ and Rh^{3+} with 30 mM DEDPPDA was heated at 356 K for 5 h. This aqueous solution was repeatedly shaken four times with fresh 1-octanol solution containing 500 mM $LiTf_2N$ for 5 min at RT.

EXPERIMENTAL SECTION

Materials. All chemicals employed in this study were of reagent grade and used as received. The water-soluble PDA ligands were prepared as follows and characterized by ^1H and $^{13}C\{^1H\}$ NMR (JEOL JNM ECX-400) and IR spectroscopy
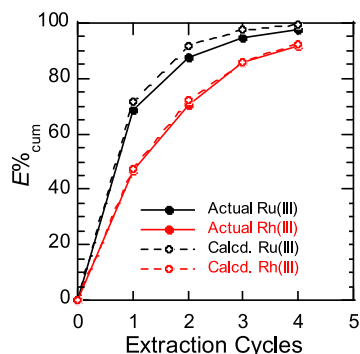
[JASCO FT/IR-4700 with diamond prism attenuated total reflection (ATR) apparatus].

Synthesis of TMPDA. Potassium carbonate (0.0962 mol, FUJIFILM Wako Pure Chemical Corporation) and dimethylamine hydrochloride (0.0193 mol, Tokyo Chemical Industry Co., Ltd.) were added to THF (40 mL, Kanto Chemical Co., Inc.) in a 100 mL round-bottom flask. The mixture was stirred at RT overnight and cooled in an ice bath. THF (5 mL) containing 2,6-pyridinedicarbonyl dichloride (0.00961 mol, Wako Chemical Ltd.) was slowly added to the mixture using a dropping funnel. Additional THF (10 mL) was then further loaded. The mixture was stirred in the ice bath for 6 h and at RT overnight. After removing the white precipitate by filtration, the supernatant was concentrated using a rotary evaporator to give a white powder of TMPDA (30% yield).

General Procedure of Synthesis of PDA Ligands. 2,6-Pyridinedicarbonyl dichloride (0.00961 mol, Wako Chemical Ltd.) and triethylamine (0.0193 mol, Kanto Chemical Co., Inc.) were dissolved in THF (40 mL, Kanto Chemical Co., Inc.) in a 100 mL round-bottom flask. After the mixture was cooled in an ice bath, THF (5 mL) containing N-ethylmethylamine, diethylamine, N-methylpropylamine, or N-ethylpropylamine (0.0192 mol, Tokyo Chemical Industry Co., Ltd.) was slowly added using a dropping funnel. Additional THF (10 mL) was then further loaded. The mixture was stirred in the ice bath for 1 h and at RT overnight. After removing the white precipitate by filtration, the supernatant was concentrated using a rotary evaporator. The residue was dissolved in dichloromethane (30 mL) and mixed with 2 M HCl(aq) (2 mL). The organic layer was separated, mixed with a small portion of K_2CO_3 and $MgSO_4$, and rested for 15 min. Then, solid materials were removed by filtration. Any volatile material in the filtrate was removed using the rotary evaporator.

Characterization of PDA Ligands. *TMPDA.* Yield: 30%, white powder. ^1H NMR (CDCl$_3$, δ/ppm vs TMS): 3.05 (s, 6H, NC$\underline{H}_3$), 3.14 (s, NC$\underline{H}_3$), 7.66 (d, J = 8.0 Hz, 2H, 3,5-H), 7.90 (t, J = 8.0 Hz, 1H, 4-H). $^{13}C\{^1H\}$ NMR (CDCl$_3$, δ/ppm vs TMS): 35.82, 39.14, 124.11, 138.16, 153.27, 168.39. IR (ATR) cm^{-1}: 1635 (>C=O).

DEDMPDA. 35%, yellow powder. ^1H NMR (CDCl$_3$, δ/ppm vs TMS): 1.16 (m, 3H, NCH$_2$C$\underline{H}_3$), 1.26 (m, 3H, NCH$_2$C$\underline{H}_3$), 3.01 (s, 3H, NC$\underline{H}_3$), 3.10 (s, 3H, NC$\underline{H}_3$), 3.36 (q, J = 6.8 Hz, 2H, NC$\underline{H}_2$CH$_3$), 3.60 (q, J = 7.2 Hz, 2H, NC$\underline{H}_2$CH$_3$), 7.64 (q, J = 8.8 Hz, 2H, 3,5-H), 7.89 (t, J = 8.0 Hz, 1H, 4-H). $^{13}C\{^1H\}$ NMR (CDCl$_3$, δ/ppm vs TMS): 12.01, 13.70, 32.90, 36.42, 42.87, 45.90, 123.95, 138.10, 153.48, 168.23. IR (ATR) cm^{-1}: 1642 (>C=O).

TEPDA. 42%, yellow powder. ^1H NMR (CDCl$_3$, δ/ppm vs TMS): 1.15 (t, J = 7.2 Hz, 6H, NCH$_2$C$\underline{H}_3$), 1.26 (t, J = 7.2 Hz, 6H, NCH$_2$C$\underline{H}_3$), 3.35 (q, J = 7.2 Hz, 4H, NC$\underline{H}_2$CH$_3$), 3.56 (q, J = 6.8 Hz, 4H, 4H, NC$\underline{H}_2$CH$_3$), 7.62 (d, J = 7.6 Hz, 2H, 3,5-H), 7.87 (t, J = 7.6 Hz, 1H, 4-H). $^{13}C\{^1H\}$ NMR (CDCl$_3$, δ/ppm vs TMS): 12.8, 14.29, 40.22, 43.32, 123.70, 138.00, 153.63, 168.13. IR (ATR) cm^{-1}: 1627 (>C=O).

DMDPPDA. 61%, yellow oil. ^1H NMR (CDCl$_3$, δ/ppm vs TMS): 0.75 (q, J = 7.6 Hz, 3H, NCH$_2$CH$_2$C$\underline{H}_3$), 0.97 (t, J = 7.2 Hz, 3H, NCH$_2$CH$_2$C$\underline{H}_3$), 1.64 (m, 4H, NCH$_2$C$\underline{H}_2$CH$_3$), 2.98 (d, J = 4 Hz, 2H, NC$\underline{H}_3$), 3.09 (d, J = 1.2 Hz, 2H, NC$\underline{H}_3$), 3.27 (q, J = 7.2 Hz, 3H, NCH$_2$CH$_2$C$\underline{H}_3$), 3.50 (t, J = 7.6 Hz, 3H, NCH$_2$CH$_2$C$\underline{H}_3$), 7.62 (t, J = 8.4 Hz, 2H, 3,5-H), 7.86 (t, J = 7.6 Hz, 1H, 4-H). $^{13}C\{^1H\}$ NMR (CDCl$_3$, δ/ppm vs TMS): 10.92, 11.33, 20.25, 21.65, 33.40, 37.12, 49.71, 52.69, 124.01, 138.07, 153.45, 168.64. IR (ATR) cm^{-1}: 1646 (>C=O).

DEDPPDA. 70%, yellow oil. ^1H NMR (CDCl$_3$, δ/ppm vs TMS): 0.74 (t, J = 7.2 Hz, 3H, NCH$_2$CH$_2$C$\underline{H}_3$), 0.97 (t, J = 7.6 Hz, 3H, NCH$_2$CH$_2$C$\underline{H}_3$), 1.11 (q, J = 7.2 Hz, 3H, NCH$_2$C$\underline{H}_3$), 1.24 (t, J = 7.2 Hz, 3H, NCH$_2$C$\underline{H}_3$), 1.61 (m, 2H, NCH$_2$C$\underline{H}_2$CH$_3$), 1.70 (m, 2H, NCH$_2$C$\underline{H}_2$CH$_3$), 3.25 (t, J = 7.6 Hz, 2H, NC$\underline{H}_2$CH$_2$CH$_3$), 3.34 (q, J = 7.2 Hz, 2H, NC$\underline{H}_2$CH$_3$), 3.45 (t, J = 6.8 Hz, 2H, NC$\underline{H}_2$CH$_2$CH$_3$), 3.54 (q, J = 7.2 Hz, 2H, NC$\underline{H}_2$CH$_3$), 7.62 (q, J = 6.8 Hz, 2H, 3,5-H), 7.85 (t, J = 7.6 Hz, 1H, 4-H). $^{13}C\{^1H\}$ NMR (CDCl$_3$, δ/ppm vs TMS): 11.09, 11.52, 12.78, 14.28, 20.83, 22.23, 40.70, 43.65, 47.07, 50.23, 123.95, 137.99, 153.63, 168.39. IR (ATR) cm^{-1}: 1642 (>C=O).

The detailed results of the characterization of PDA ligands are reported in Supporting Information.

Measurement of the Partition Coefficient of PDA Ligands. The pre-equilibrated 1-octanol containing TMPDA, DEDMPDA, TEPDA, DMDPPDA, DEDPPDA, and TBPDA (30 mM) was mixed with the pre-equilibrated 0.5 M HNO$_3$(aq), respectively. The volume ratio between aqueous and organic phases was always maintained at 1:1. After 30 min mixing for equilibration, the organic layer (630 μL) was mixed with a methanol-d_4 solution (70 μL) dissolving a standard material (benzyl bromide). Concentrations of PDA ligands in the organic layer were determined by ^1H NMR peak integrals compared with that of benzyl bromide as a reference. The value of log P of the PDA ligand was calculated as follows.

$$\log P = \log([\text{PDA}]_{\text{org}}/[\text{PDA}]_{\text{aq}}) \quad (15)$$

$$[\text{PDA}]_{\text{aq}} = [\text{PDA}]_{\text{ini}} - [\text{PDA}]_{\text{org}} \quad (16)$$

where $[\text{PDA}]_{\text{org}}$ and $[\text{PDA}]_{\text{aq}}$ denote the concentrations of PDA ligands in the organic phase and the aqueous phase after equilibration, respectively. $[\text{PDA}]_{\text{ini}}$ denotes the concentrations of PDA ligands in the organic phase at the initial state.

Measurement of Solubility of PDA Ligands. TMPDA, DEDMPDA, TEPDA, DMDPPDA, DEDPPDA, and TBPDA were added to 0.5 M HNO$_3$(aq) solutions, respectively, until deposition was observed. After the solutions were centrifuged, supernatants were mixed with sodium acetate aqueous solution as a reference and deuterium oxide. Concentrations of PDA ligands in the mixture were determined by ^1H NMR peak integrals compared with that of sodium acetate as a reference.

Single-Element Extraction of Ru(III) and Rh(III). The pre-equilibrated 0.5 M HNO$_3$(aq) containing a metal ion (M) like 5 mM Ru(NO)$^{3+}$ or 5 mM Rh^{3+} was loaded into a plastic tube with the PDA ligand. The aqueous solution was heated at 356 K for 5 h in an aluminium block dry bath (ASONE-THB-1). After cooling to RT, the aqueous solution was mixed with a pre-equilibrated organic solvent (1-octanol) containing LiTf$_2$N. The volume ratio between aqueous and organic phases was always maintained at 1:1. The mixture was shaken at 1500 rpm in a high-speed shaker for 5 min. For analysis, a small amount of mixture was centrifuged. The M concentration in the aqueous layer was determined by ICP-AES (Thermo Scientific iCAP7200 Duo). The values of E % and D were calculated as follows.

$$E \% = 100 \times ([\text{M}]_{\text{ini}} - [\text{M}]_{\text{aq}})/[\text{M}]_{\text{ini}} \quad (17)$$

$$D = ([\text{M}]_{\text{ini}} - [\text{M}]_{\text{aq}})/[\text{M}]_{\text{aq}} \quad (18)$$

where $[M]_{ini}$ and $[M]_{aq}$ denote the metal concentrations in the aqueous phase at the initial state and after the extraction, respectively.

Multistage Extraction of Mixture of Ru(III) and Rh(III). The pre-equilibrated 0.5 M HNO_3(aq) containing 5 mM $Ru(NO)^{3+}$ and 5 mM Rh^{3+} was loaded into a plastic tube with a 30 mM DEDPPDA ligand. The aqueous solution was heated at 356 K in a dry bath for 5 h. After cooling to RT, the aqueous solution was mixed with a pre-equilibrated organic solvent (1-octanol) containing 500 mM $LiTf_2N$. The volume ratio between aqueous and organic phases was always maintained at 1:1. The mixture was shaken at 1500 rpm in a high-speed shaker for 5 min at RT and was centrifuged. After separation of the organic layer, the aqueous phase was separated from the mixture and repeatedly stirred with same but fresh organic solvent. This distribution process was repeated four times. For analysis, a small amount of the mixture after each distribution process was centrifuged. The M concentration in the aqueous layer was determined by ICP-AES (Thermo Scientific iCAP7200 Duo). The value of $E \%_{cum}$ at each extraction stage was calculated as follows.

$$E \%_{cum} = 100 \times ([M]_{ini} - [M]_{(n \text{ cycle})aq})/[M]_{ini} \quad (19)$$

where $[M]_{ini}$ denotes the metal concentrations in the aqueous phase at the initial state and $[M]_{(n \text{ cycle})aq}$ denotes the metal concentration in the aqueous phase after n extraction cycle (n = 1−4).

Single-Crystal X-ray Diffraction. A single crystal of the $[Ru(NO)]^{3+}$ complex with 2,6-pyridinedicarboxylate and 6-(diethylcarbamoyl)picolinate deposited in the NMR sample tube was mounted on a Kapton capillary equipped with the goniometer head. Intensity data were collected using Rigaku XtaLAB mini II with graphite monochromated Mo Kα radiation (λ = 0.71075 Å). The obtained diffraction data were analyzed by Olex2 software package[22] suited with SHELX. The structure was solved by SHELXS or SHELXT[23,24] and expanded using Fourier techniques. All non-hydrogen atoms were anisotropically refined by SHELXL 2017/1. Hydrogen atoms were refined as riding on their parent atoms with $U_{iso}(H) = 1.2U_{eq}(C)$. The final cycle of the full-matrix least-squares refinement on F^2 was based on the observed reflections and parameters and converged with the unweighted and weighted agreement factors, R and wR, respectively. The crystallographic data were described in the caption of Figure S28.

ASSOCIATED CONTENT

Ⓢ Supporting Information

The Supporting Information is available free of charge at https://pubs.acs.org/doi/10.1021/acsomega.1c03565.

> Progress of absorbance as a function of elapsed time for UV−vis absorption spectra at 356 K, UV−vis absorption spectra at 298 K for Ru(III) and Rh(III) systems, effects of log[TEPDA] and log[Tf_2N^-] to log D of $Ru(NO)^{3+}$ and Rh^{3+}, calculated logarithmic gross stability constant (log β_n) of $[Ru(NO)(TEPDA)_n]^{3+}$ and $[Rh(TEPDA)_n]^{3+}$, ^1H NMR spectra of TEPDA and its predictable decomposition products, ORTEP drawing of $Ru(NO)^{3+}$ complex with 2,6-pyridinedicarboxylate and 6-(diethylcarbamoyl)picolinate, and ^1H NMR, $^{13}C\{^1H\}$ NMR, and IR spectra of PDA ligands (PDF)
>
> Crystallographic data of $Ru(NO)^{3+}$ complex (CIF)

Accession Codes

CCDC 2072310 contains the supplementary crystallographic data for this paper. This data can be obtained free of charge via www.ccdc.cam.ac.uk/data_request/cif, or by emailing data_request@ccdc.cam.ac.uk, or by contacting The Cambridge Crystallographic Data Centre, 12 Union Road, Cambridge CB2 1EZ, UK; fax: +44 1223 336033.

AUTHOR INFORMATION

Corresponding Author

Koichiro Takao − *Laboratory for Zero-Carbon Energy, Institute of Innovative Research, Tokyo Institute of Technology, 152-8550 Tokyo, Japan;* ⦿ orcid.org/0000-0002-0952-1334; Email: takao.k.ac@m.titech.ac.jp

Authors

Zhiwei Zheng − *Laboratory for Zero-Carbon Energy, Institute of Innovative Research, Tokyo Institute of Technology, 152-8550 Tokyo, Japan;* ⦿ orcid.org/0000-0001-8792-1774

Tsuyoshi Arai − *Graduate School of Engineering, Shibaura Institute of Technology, 135-8548 Tokyo, Japan*

Complete contact information is available at:
https://pubs.acs.org/10.1021/acsomega.1c03565

Author Contributions

This article was submitted and published with the consent of all authors. Z.Z. conducted all experiments and manuscript preparation under supervision by K.T. Also, T.A. significantly contributed to most discussion and data interpretations.

Notes

The authors declare no competing financial interest.

REFERENCES

(1) Rao, C. R. M.; Reddi, G. S. Platinum group metals (PGM); occurrence, use and recent trends in their determination. *Trends Anal. Chem.* **2000**, *19*, 565−586.

(2) Gerst, M. D.; Graedel, T. E. In-Use Stocks of Metals: Status and Implications. *Environ. Sci. Technol.* **2008**, *42*, 7038−7045.

(3) Fornalczyk, A. Industrial Catalysts as a Source of Valuable Metals. *J. Achiev. Mater. Manuf. Eng.* **2012**, *55*, 864−869.

(4) Newman, R. J.; Smith, F. J. Platinum Metals from Nuclear Fission. *Platin. Met. Rev.* **1970**, *14*, 88−92.

(5) Kolarik, Z.; Renard, E. V. Recovery of Value Fission Platinoids from Spent Nuclear Fuel. *Platin. Met. Rev.* **2003**, *47*, 74−87.

(6) Kolliopoulos, G.; Balomenos, E.; Giannopoulou, I.; Yakoumis, I.; Panias, D. Behavior of Platinum Group Metals during Their Pyrometallurgical Recovery from Spent Automotive Catalysts. *Open Access Lib. J.* **2014**, *1*, No. e736.

(7) Steinlechner, S.; Antrekowitsch, J. Potential of a Hydrometallurgical Recycling Process for Catalysts to Cover the Demand for Critical Metals, Like PGMs and Cerium. *JOM* **2015**, *67*, 406−411.

(8) Helm, L.; Merbach, A. E. Inorganic and bioinorganic solvent exchange mechanisms. *Chem. Rev.* **2005**, *105*, 1923−1960.

(9) Ikeda, S.; Mori, T.; Ikeda, Y.; Takao, K. Microwave-Assisted Solvent Extraction of Inert Platinum Group Metals from HNO_3(aq)

to Betainium-Based Thermomorphic Ionic Liquid. *ACS Sustainable Chem. Eng.* **2016**, *4*, 2459−2463.

(10) Kono, S.; Kazama, H.; Mori, T.; Arai, T.; Takao, K. Significant Acceleration of PGMs Extraction with UCST-type Thermomorphic Ionic Liquid at Elevated Temperature. *ACS Sustainable Chem. Eng.* **2018**, *6*, 1555−1559.

(11) Zheng, Z.; Arai, T.; Takao, K. Kinetic and Thermodynamic Requirements to Extend Solvent Compatibility in Thermal-Assisted Extraction of Inert Platinum Group Metals. *ACS Sustainable Chem. Eng.* **2019**, *7*, 9750−9753.

(12) Leo, A.; Hansch, C.; Elkins, D. Partition coefficients and their uses. *Chem. Rev.* **1971**, *71*, 525−616.

(13) Mannhold, R.; Rekker, R. F. The hydrophobic fragmental constant approach for calculating log P in octanol/water and aliphatic hydrocarbon/water systems. *Perspect. Drug Discovery Des.* **2000**, *18*, 1−18.

(14) Rose, M. J.; Fry, N. L.; Marlow, R.; Hinck, L.; Mascharak, P. K. Sensitization of Ruthenium Nitrosyls to Visible Light via Direct Coordination of the Dye Resorufin: Trackable NO Donors for Light Triggered NO Delivery to Cellular Targets. *J. Am. Chem. Soc.* **2008**, *130*, 8834−8846.

(15) Yoshida, W.; Baba, Y.; Kubota, F.; Kamiya, N.; Goto, M. Extraction and Stripping Behavior of Platinum Group Metals Using an Amic-Acid-Type Extractant. *J. Chem. Eng. Jpn.* **2017**, *50*, 521−526.

(16) Tomitaro, I.; Yoshii, K.; Yoshie, U. Solvent-Extraction Behavior of Carrier-Free Rhodium. *Bull. Chem. Soc. Jpn.* **1968**, *41*, 1458−1459.

(17) Wu, H.; Kim, S.-Y.; Takahashi, T.; Oosugi, H.; Ito, T.; Kanie, K. Extraction behaviors of platinum group metals in simulated high-level liquid waste by a hydrophobic ionic liquid bearing an amino moiety. *Nucl. Eng. Technol.* **2021**, *53*, 1218−1223.

(18) Sasaki, K.; Takao, K.; Suzuki, T.; Mori, T.; Arai, T.; Ikeda, Y. Extraction of Pd(II), Rh(III) and Ru(III) from HNO_3 aqueous solution to betainium bis(trifluoromethanesulfonyl)imide ionic liquid. *Dalton Trans.* **2014**, *43*, 5648−5651.

(19) Swain, P.; Mallika, C.; Srinivasan, R.; Mudali, U. K.; Natarajan, R. Separation and recovery of ruthenium: a review. *J. Radioanal. Nucl. Chem.* **2013**, *298*, 781−796.

(20) Lefebvre, C.; Dumas, T.; Charbonnel, M.-C.; Solari, P. L. Speciation of ruthenium in TBP/TPH organic phases: a study about acidity of nitric solutions. *Procedia Chem.* **2016**, *21*, 54−60.

(21) Caminiti, R.; Atzei, D.; Cucca, P.; Anedda, A.; Bongiovanni, G. Structure of rhodium(III) nitrate aqueous solutions. An investigation by x-ray diffraction and Raman spectroscopy. *J. Phys. Chem.* **1986**, *90*, 238−243.

(22) Dolomanov, O. V.; Bourhis, L. J.; Gildea, R. J.; Howard, J. A. K.; Puschmann, H. OLEX2: A Complete Structure Solution, Refinement and Analysis Program. *J. Appl. Crystallogr.* **2009**, *42*, 339−341.

(23) Sheldrick, G. M. SHELXT—Integrated space-group and crystal-structure determination. *Acta Crystallogr., Sect. A: Found. Adv.* **2015**, *71*, 3−8.

(24) Sheldrick, G. M. Crystal structure refinement with SHELXL. *Acta Crystallogr., Sect. C: Struct. Chem.* **2015**, *71*, 3−8.